GENETICS

Parental mutations influence wild-type offspring via transcriptional adaptation

Zhen Jiang[1,2,3]*†, Mohamed A. El-Brolosy[1,2]†‡, Vahan Serobyan[1,2,3]†, Jordan M. Welker[1,2], Nicholas Retzer[1,2], Christopher M. Dooley[1,2], Gabrielius Jakutis[1,2], Thomas Juan[1,2], Nana Fukuda[1,2], Hans-Martin Maischein[1,2], Darius Balciunas[4,5], Didier Y.R. Stainier[1,2,3]*

Transgenerational epigenetic inheritance (TEI) is mostly discussed in the context of physiological or environmental factors. Here, we show intergenerational and transgenerational inheritance of transcriptional adaptation (TA), a process whereby mutant messenger RNA (mRNA) degradation affects gene expression, in nematodes and zebrafish. Wild-type offspring of animals heterozygous for mRNA-destabilizing alleles display increased expression of adapting genes. Notably, offspring of animals heterozygous for nontranscribing alleles do not display this response. Germline-specific mutations are sufficient to induce TA in wild-type offspring, indicating that, at least for some genes, mutations in somatic tissues are not necessary for this process. Microinjecting total RNA from germ cells of TA-displaying heterozygous zebrafish can trigger TA in wild-type embryos and in their progeny, suggesting a model whereby mutant mRNAs in the germline trigger a TA response that can be epigenetically inherited. In sum, this previously unidentified mode of TEI reveals a means by which parental mutations can modulate the offspring's transcriptome.

INTRODUCTION

Inheritance is the process by which traits or information is transmitted from one generation to the next. The classical view of genetic inheritance involves the transmission of DNA from parents to their offspring (*1*). However, a number of studies have reported examples of heritable phenotypic variations that cannot be explained solely by the genetic makeup of the parents (*2*–*4*). Multigenerational "non-genetic" inheritance in mammals can refer to bioactive substances, such as hormones and cytokines, being passed across generations without the involvement of the gametes (*5*); however, it more commonly refers to intergenerational epigenetic inheritance (IEI) or transgenerational epigenetic inheritance (TEI), which describe the transmission of epigenetic information from the gametes to the zygote (*3*, *6*). By definition, epigenetic inheritance occurs independently of the progeny's genomic sequence (*5*). When the effects can be detected in the second and subsequent generations after the initial trigger (i.e., P0 to F1 to F2 and so on), this phenomenon is referred to as transgenerational inheritance; when the inheritance mode only lasts for one generation, it is referred to as intergenerational inheritance (i.e., P0 to F1) (*7*). Nevertheless, several studies have suggested that intergenerational and transgenerational effects share underlying mechanisms [reviewed in (*7*–*9*)]. A range of studies have provided evidence that physiological and environmental factors can modulate the inheritance of transgenerational traits through epigenetic mechanisms including DNA methylation, histone modifications, and noncoding RNAs (*8*, *10*–*15*). Indeed, RNA-induced epigenetic modifications are now a well-documented phenomenon (*16*–*18*). Intriguingly, several studies in mouse have reported heterozygous traits in wild-type offspring of heterozygous parents (*19*, *20*), a phenomenon attributed to paramutations, i.e., interactions between two alleles at a single locus whereby one allele induces a heritable change in the other allele. While studies reporting paramutations in plants (i.e., originally in maize) (*21*), *Caenorhabditis elegans* (*22*), and *Drosophila melanogaster* (*23*) suggest that parental genotype can influence the offspring's traits independent of the offspring's genotype, the underlying mechanisms remain largely unknown. Despite the increased discussion of the role of physiologically and environmentally induced IEI/TEI and their potential influence on genetic robustness and plasticity (*3*, *11*, *15*, *24*–*27*), it remains unclear how often inter-/transgenerational effects are adaptive. Furthermore, the potential role of IEI/TEI to achieve robustness in the face of parental genetic alterations has not yet been reported.

Transcriptional adaptation (TA), a newly identified cellular response to some genetic perturbations, refers to the phenomenon whereby a mutation in one gene triggers the transcriptional modulation of other genes, termed adapting genes (*28*–*30*). In zebrafish, in mouse cells in culture, and in *C. elegans*, mutations leading to mutant mRNA degradation, including those leading to a premature termination codon (PTC), can induce the up-regulation of adapting genes (*28*–*30*), whereas mutations leading to the absence of mRNA (i.e., promoter deletions or full-locus deletions that lead to nontranscribing, or RNA-less, alleles) do not (*28*, *30*), indicating that transcripts from the mutated locus are required for TA (*28*–*30*). Further data indicate that mutant mRNA degradation is required for TA (*28*, *30*). Changes in chromatin modifications have also been observed during the TA response, as increased levels of the H3K4me3 histone mark were detected at the promoter region of the adapting genes in a mouse cell line TA model (*28*) and in a zebrafish TA model (*29*), suggesting that chromatin alteration is involved in the up-regulation of the adapting genes. Thus, the mutant mRNA (*29*), its degradation products (*28*), or their derivatives, could lead to a modified chromatin state at the adapting gene loci.

In this study, we investigated how a mutation in an ancestral genome can influence the offspring's transcriptional landscape and thus possibly promote genetic robustness. We found that wild-type offspring of TA-displaying heterozygous animals exhibit increased

[1]Max Planck Institute for Heart and Lung Research, Department of Developmental Genetics, Bad Nauheim, Germany. [2]German Centre for Cardiovascular Research (DZHK), Partner Site Rhine-Main, Bad Nauheim, Germany. [3]Cardio-Pulmonary Institute (CPI), Bad Nauheim, Germany. [4]Department of Biology, College of Science and Technology, Temple University, Philadelphia, PA, USA. [5]Life Sciences Centre, Vilnius University, Vilnius, Lithuania.
*Corresponding author. Email: didier.stainier@mpi-bn.mpg.de (D.Y.R.S.); jane.jiang@mpi-bn.mpg.de (Z.J.)
†These authors contributed equally to this work.
‡Present address: Society of Fellows, Harvard University, Cambridge, MA, USA.

expression of the adapting genes and term this phenomenon intergenerational and transgenerational inheritance of TA (IGTA and TGTA). TGTA in zebrafish can be observed for at least two generations and in *C. elegans* for at least nine generations. Microinjections into one-cell stage zebrafish embryos of total RNA from germ cells of TA-displaying heterozygotes can induce TA and IGTA. These data suggest that germline transmission of RNA, potentially the mutant mRNA and/or its degradation products (or their derivatives), can underlie the inheritance of TA. We also observed TA in the wild-type progeny of animals with a germline-specific *aldh1a2* PTC mutation, further highlighting the key role of the germline in IGTA.

RESULTS

Transgenerational inheritance of the transcriptional adaptation response in *C. elegans* and zebrafish

We previously reported that, in *C. elegans*, *act-3* mRNA levels were up-regulated in *act-5(dt2019)* mutants, hereafter referred to as *act-5(ptc)* (*30*). In addition, the expression pattern of an extrachromosomal *act-3p::rfp* reporter (i.e., a 4.5-kb *act-3* enhancer/promoter fragment driving *rfp* expression) in *act-5(ptc)* mutants was altered compared with that in wild-type nematodes or in an *act-5(deletion)* mutant allele that does not display TA (*30*). We observed red fluorescent protein (RFP) expression in the pharynx in *act-5(+/+); Ex[act-3p::rfp]* nematodes and in the pharynx and intestine in *act-5(ptc/ptc);Ex[act-3p::rfp]* nematodes (*30*). As we attempted to use this phenotype [RFP expression in the intestine of *act-5(ptc)* mutants] in a forward genetic screen for regulators of TA, we observed that 100% of the *act-5(+/+);Ex[act-3p::rfp]* offspring from *act-5(ptc)* heterozygous nematodes displayed intestinal RFP expression (Fig. 1, A and B). To further analyze the inheritance mode of this phenotype, we sequentially self-fertilized wild-type hermaphrodite offspring from *act-5(ptc)* heterozygous nematodes and observed the intestinal expression of the *act-3p::rfp* reporter up to six generations (Fig. 1B).

In addition, we generated an allele (*Si[eft-3p::act-5(ptc)]*) that expresses an *act-5(ptc)* transgene under the control of an *eft-3* promoter via Mos1-mediated single-copy insertion (*31*). We observed increased *act-3* mRNA levels in these transgenic animals (fig. S1A), and when we generated an *Ex[act-3p::rfp]* reporter line in this background (i.e., *Si[eft-3p::act-5(ptc)](tg/tg);Ex[act-3p::rfp]*), we observed ectopic RFP expression in their uterus, a tissue that expresses *eft-3* (*32*). These data indicate that overexpressing an *act-5(ptc)* transgene can trigger TA. Similar to our observations with *act-5(+/+);Ex[act-3p::rfp]* nematodes, we observed that 100% of the wild-type *Ex[act-3p::rfp]* offspring from *Si[eft-3p::act-5(ptc)](tg/+);Ex[act-3p::rfp]* nematodes displayed ectopic RFP expression in their uterus (fig. S1, B and C), and this phenotype was observed across nine generations (Fig. 1, C and D). Together, these data show that the TA-induced ectopic RFP expression in both *act-5(ptc);Ex[act-3p::rfp]* and *Si[eft-3p::act-5(ptc)](tg/+);Ex[act-3p::rfp]* nematodes is inherited transgenerationally, revealing TGTA in *C. elegans*.

In zebrafish, the previously reported *alcama*, *vcla*, and *egfl7* PTC-bearing mutants exhibit a decrease in mutant mRNA levels and an increase in mRNA levels of the adapting genes, namely, *alcamb*, *vclb*, and *emilin2a/emilin3a*, respectively (*28*, *33*). In addition to these published models, we also introduce here an *aldh1a2* PTC-containing allele (*34*) as another TA model that exhibits decreased mutant mRNA levels and increased *aldh1a3* mRNA levels (fig. S2A). Injection of wild-type *aldh1a2* mRNA into *aldh1a2* mutants did not affect the up-regulation of *aldh1a3* (fig. S2B), indicating that it is triggered independently of the loss of Aldh1a2 protein and thus a TA model. In addition, a similar increase in *aldh1a3* mRNA levels was observed in *aldh1a2*$^{floxed/+}$ embryos upon *Cre* mRNA-mediated recombination (fig. S2, C and D), which leads to the same PTC as in the *aldh1a2*^{ptc} allele (*34*).

To investigate whether zebrafish exhibit IGTA, we first determined the mRNA levels of the adapting genes in wild-type offspring from PTC-allele heterozygous intercrosses (Fig. 2A) (see Materials and Methods) compared with their levels in embryos obtained from incrosses of the corresponding wild-type strain (AB or TL). Notably, we observed increased mRNA levels of the adapting genes, *alcamb*, *vclb*, *emilin2a/emilin3a*, and *adh1a3*, in the wild-type offspring from intercrosses of *alcama*, *vcla*, *egfl7*, and *aldh1a2* heterozygous zebrafish, respectively (Fig. 2, B to E, and fig. S2E). To test whether this increase in mRNA levels of the adapting genes was triggered by the inheritance of the TA response, we analyzed wild-type offspring from *alcama* and *egfl7* RNA-less allele heterozygous intercrosses and observed no significant up-regulation of the adapting genes (fig. S3, A and B). In addition, we generated an RNA-less allele of *vcla* (a 72.44-kb deletion that removes the *vcla* locus; fig. S3, C and D) and found that it does not display TA (fig. S3E). We also analyzed wild-type offspring from *vcla* RNA-less allele heterozygous intercrosses and observed no increased expression of the adapting gene when compared with embryos obtained from AB incrosses (fig. S3F). Together, these data indicate that the parents need to experience TA for the inheritance of the TA response to occur. Furthermore, we observed a significant increase in the mRNA levels of the adapting genes in second-generation wild-type embryos (F2) from F1 *alcama*$^{+/+}$, *vcla*$^{+/+}$, *egfl7*$^{+/+}$, and *aldh1a2*$^{+/+}$ incrosses (Fig. 2, F to I, and fig. S2F), indicating that, similar to the situation in *C. elegans*, TGTA is also observed in zebrafish. To begin to examine the specificity of TGTA, we measured *alcamb* mRNA levels in second-generation wild-type embryos (F2) from F1 *egfl7*$^{+/+}$ incrosses and observed no significant difference compared with wild-type embryos from AB incrosses (fig. S3G).

Next, we investigated whether parental gender was an important factor in IGTA. We crossed male and female heterozygous zebrafish to wild types and examined the mRNA levels of the adapting genes. We observed an increase in *alcamb* mRNA levels in the wild-type offspring from *alcama*$^{ptc/+}$ male outcrosses but not from *alcama*$^{ptc/+}$ female outcrosses at 28 hours postfertilization (hpf) (fig. S4, A and B); however, when we analyzed pre-mRNA levels in such embryos at 6 hpf, we observed significant up-regulation of *alcamb* in the wild-type offspring from both male and female outcrosses (fig. S4, C and D), suggesting an increase in transcription of the adapting gene and an involvement of gender-specific posttranscriptional regulation. However, for the *egfl7*^{ptc} model, we observed, at 24 hpf, an increase in *emilin2a* mRNA levels in the wild-type offspring from both male and female outcrosses (fig. S4, E and F).

To determine whether the increase in mRNA levels observed during TGTA was due to increased transcription or increased mRNA stability, we performed metabolic labeling of newly synthesized transcripts. We observed significantly increased transcription of the adapting genes *alcamb*, *emilin2a*, *vclb*, and *aldh1a3* in second-generation wild-type embryos (F2) obtained from F1 *alcama*$^{+/+}$, *egfl7*$^{+/+}$, *vcla*$^{+/+}$, and *aldh1a2*$^{+/+}$ incrosses (fig. S5), respectively. Thus, TGTA, like TA, occurs due to increased transcription, not increased mRNA stability.

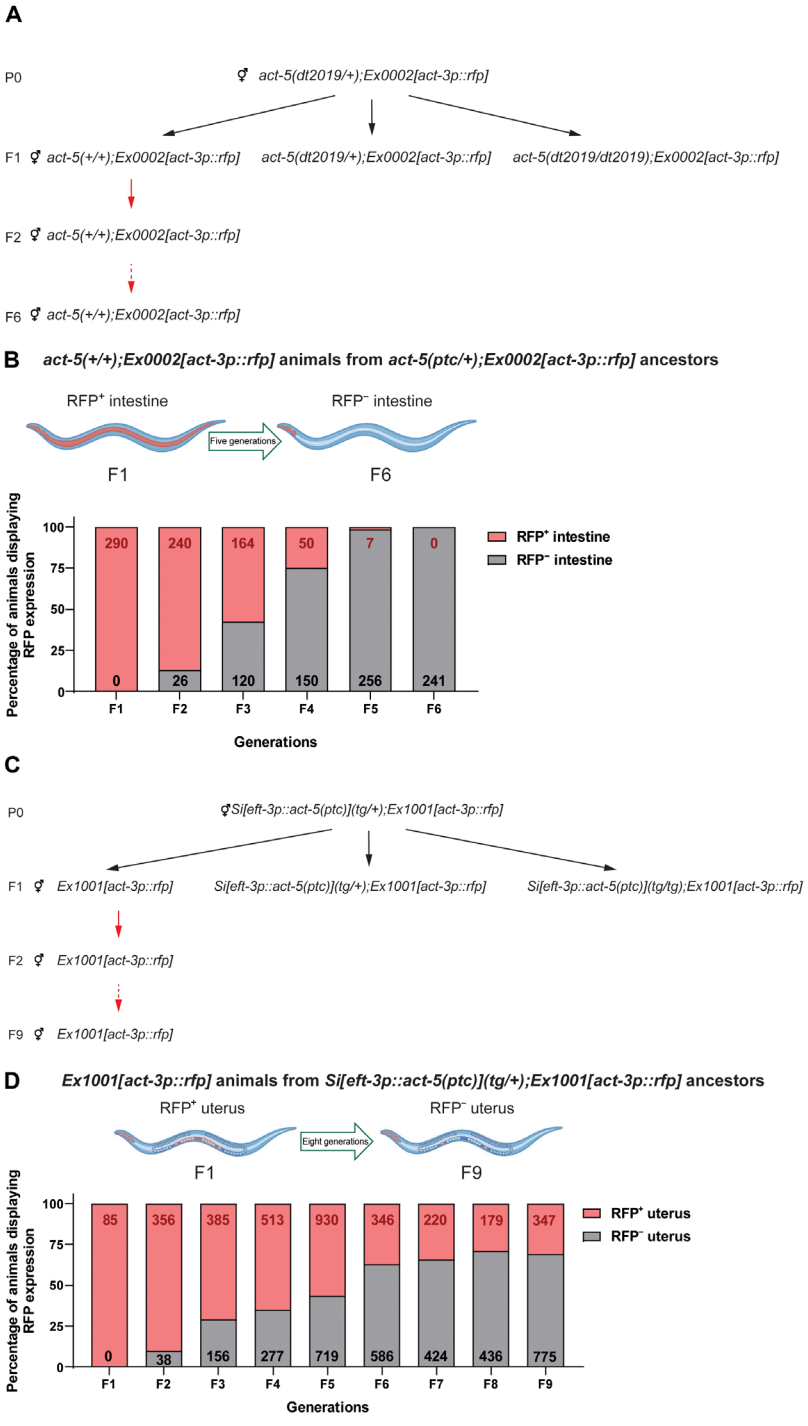

Fig. 1. TGTA in *C. elegans*. (**A**) Genetic crosses used to obtain *Ex0002[act-3p::rfp]* wild-type offspring from *act-5(dt2019);Ex0002[act-3p::rfp]* heterozygous nematodes. Black arrows indicate the self-fertilization of hermaphrodites; red arrows indicate subsequent wild-type self-crosses. (**B**) Percentage of adult *Ex0002[act-3p::rfp]* wild-type nematodes displaying ectopic red fluorescent protein (RFP) expression in their intestine through six generations from *act-5(dt2019/+);Ex0002[act-3p::rfp]* ancestors. Red numbers indicate the total number of *Ex0002[act-3p::rfp]* wild-type nematodes displaying ectopic RFP expression in their intestine in each generation; black numbers indicate the total number of *Ex0002[act-3p::rfp]* wild-type nematodes displaying pharynx-only RFP expression in each generation. (**C**) Genetic crosses used to obtain *Ex1001[act-3p::rfp]* offspring from *Si[eft-3p::act-5(ptc)](tg/+);Ex1001[act-3p::rfp]* nematodes. Black arrows indicate the self-fertilization of hermaphrodites; red arrows indicate subsequent wild-type self-crosses. (**D**) Percentage of adult *Ex1001[act-3p::rfp]* wild-type nematodes displaying ectopic RFP expression in their uterus through nine generations from *Si[eft-3p::act-5(ptc)](tg/+);Ex1001[act-3p::rfp]* ancestors. Red numbers indicate the total number of *Ex1001[act-3p::rfp]* wild-type nematodes displaying ectopic RFP expression in their uterus in each generation; black numbers indicate the total number of *Ex1001[act-3p::rfp]* wild-type nematodes displaying only pharynx and spermatheca RFP expression (fig. S1D) in each generation. Illustrations were created with BioRender.com.

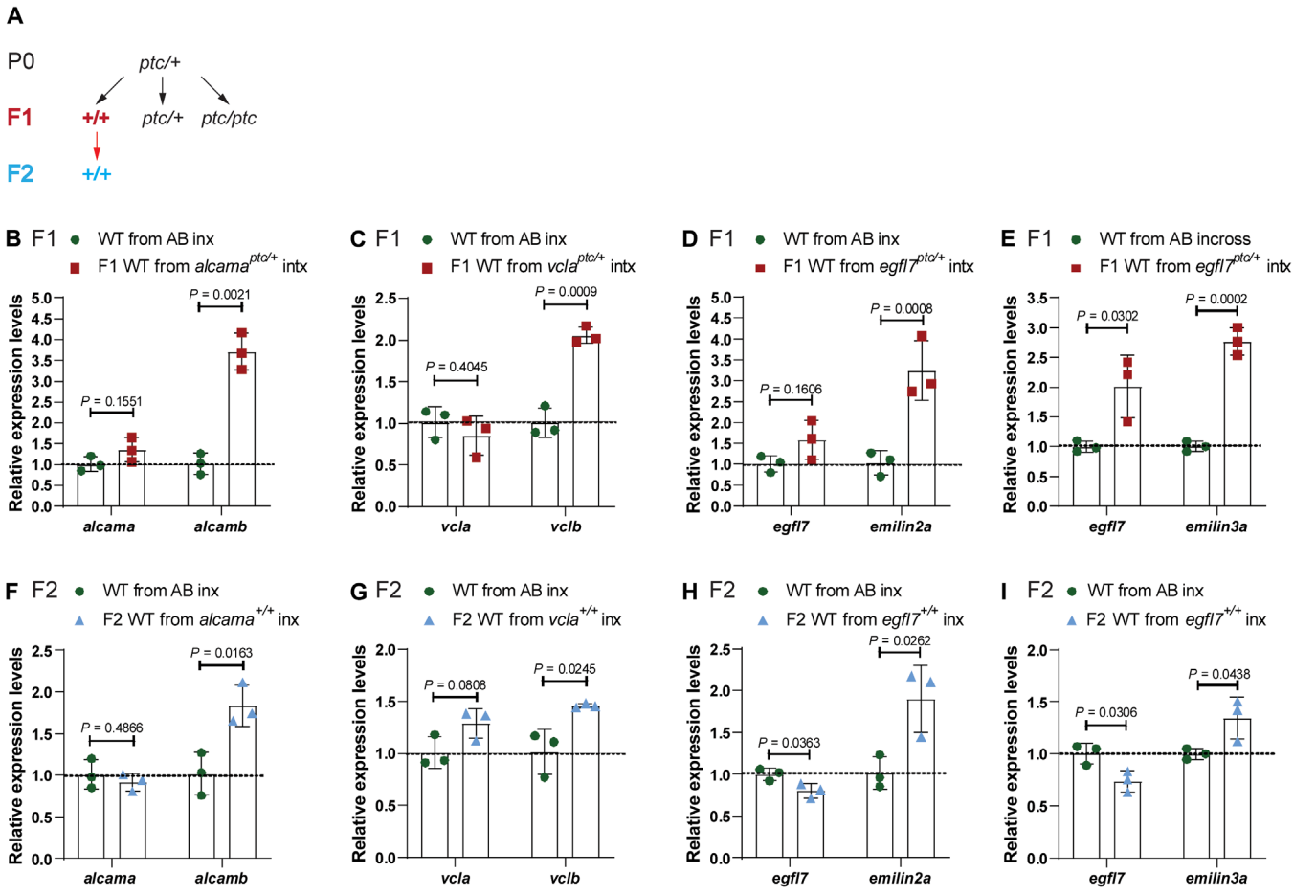

Fig. 2. TGTA in zebrafish. (**A**) Genetic crosses used to obtain wild-type (WT) embryos from TA-displaying heterozygous zebrafish and from subsequent incrosses. Black arrows indicate heterozygous intercrosses (intx); red arrow indicates subsequent wild-type incrosses (inx). (**B**) Relative mRNA levels of *alcama* and *alcamb* in 28 hpf wild-type embryos from AB incrosses and from *alcama*$^{ptc/+}$ intercrosses. (**C**) Relative mRNA levels of *vcla* and *vclb* in 24 hpf wild-type embryos from AB incrosses and *vcla*$^{ptc/+}$ intercrosses. (**D**) Relative mRNA levels of *egfl7* and *emilin2a* in 24 hpf wild-type embryos from AB incrosses and *egfl7*$^{ptc/+}$ intercrosses. (**E**) Relative mRNA levels of *egfl7* and *emilin3a* in 24 hpf wild-type embryos from AB incrosses and *egfl7*$^{ptc/+}$ intercrosses. (**F**) Relative mRNA levels of *alcama* and *alcamb* in 28 hpf wild-type embryos obtained from AB incrosses and F1 *alcama*$^{+/+}$ (i.e., wild types from *alcama*$^{ptc/+}$ intercrosses) incrosses. (**G**) Relative mRNA levels of *vcla* and *vclb* in 24 hpf wild-type embryos obtained from AB incrosses and F1 *vcla*$^{+/+}$ (i.e., wild types from *vcla*$^{ptc/+}$ intercrosses) incrosses. (**H**) Relative mRNA levels of *egfl7* and *emilin2a* in 24 hpf wild-type embryos obtained from AB incrosses and F1 *egfl7*$^{+/+}$ (i.e., wild types from *egfl7*$^{ptc/+}$ intercrosses) incrosses. (**I**) Relative mRNA levels of *egfl7* and *emilin3a* in 24 hpf wild-type embryos obtained from AB incrosses and F1 *egfl7*$^{+/+}$ (i.e., wild types from *egfl7*$^{ptc/+}$ intercrosses) incrosses. $n = 3$ biologically independent samples. Control expression levels were set at 1. Data are means ± SD, and a two-tailed Student's *t* test was used to calculate *P* values. *C*t values are listed in table S1.

Given the importance of the germline in the transmission of information from one generation to the next, we first examined and found germline expression of the mutated gene for all four zebrafish TGTA models (fig. S6), in agreement with a recent publication (*35*), leading us to test the role of the germline in TA and its inheritance. To generate a germline-specific mutation, we used the *aldh1a2*-floxed allele in combination with *vasa-GFP-nos1 3′UTR* and *vasa-Cre-nos1 3′UTR*. These fusions of *vasa* and *GFP/Cre* followed by the 3′ untranslated region (3′UTR) of *nos1* stabilize the mRNA in perinuclear granules (*36*), which are only present in primordial germ cells (*37*) (fig. S7, A to C'). Analysis of *vasa-GFP-nos1 3′UTR* and *vasa-Cre-nos1 3′UTR* mRNA-coinjected embryos from *aldh1a2*$^{floxed/+}$ intercrosses at 24 hpf confirmed that recombination occurred in germ cells and not in somatic cells (fig. S7, D to F), and the embryos were then raised to adulthood (Fig. 3A). Wild-type offspring from intercrosses of *vasa-Cre-nos1 3′UTR* mRNA-injected *aldh1a2*$^{floxed/+}$ zebrafish displayed significant up-regulation of *aldh1a3* mRNA levels (Fig. 3B), indicating that a germline mutation alone can be sufficient to trigger TA in wild-type offspring. To determine whether IGTA occurs in somatic cells or whether it is confined to germ cells, a *dnd1* morpholino, used to block primordial germ cell development (*38*), and *vasa-GFP-nos1 3′UTR* mRNA were coinjected into wild-type embryos and embryos from *alcama*$^{ptc/+}$ intercrosses (fig. S8, A to D). Significant up-regulation of the adapting gene was observed in the *dnd1* morpholino–injected wild-type embryos from *alcama*$^{ptc/+}$ intercrosses at 28 hpf (fig. S8E), indicating that IGTA can be detected in somatic cells.

Total RNA from germ cells of heterozygous zebrafish can trigger the transcriptional adaptation response

Because the mutated genes are expressed in the germline, we considered the possibility that transfer of RNA to the next generations

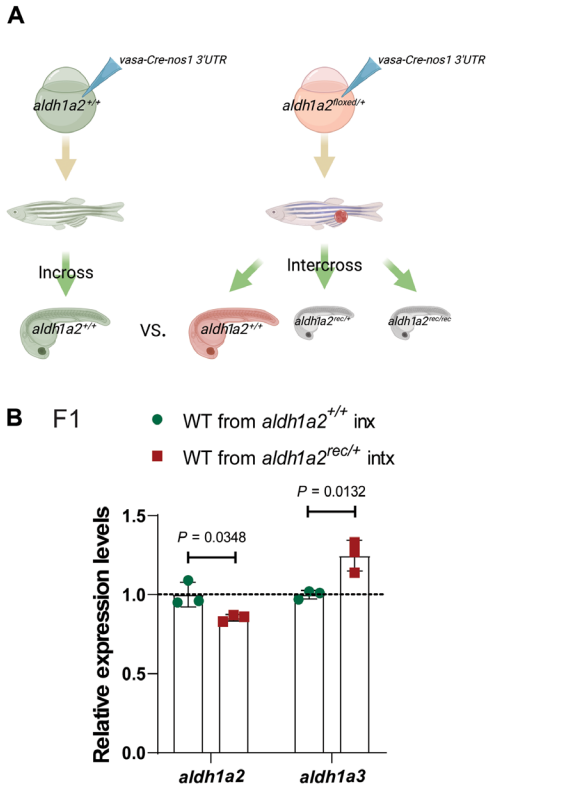

Fig. 3. The germline plays a key role in IGTA in zebrafish. (**A**) Schematic representation of experimental setup and genetic crosses used to obtain wild-type offspring; red cell indicates a germline-specific mutation. (**B**) Relative mRNA levels of *aldh1a2* and *aldh1a3* in 24 hpf wild-type embryos from *aldh1a2*$^{+/+}$ incrosses (inx) and *aldh1a2*$^{rec/+}$ intercrosses (intx). Control expression levels were set at 1. $n = 3$ biologically independent samples. Data are means ± SD, and a two-tailed Student's *t* test was used to calculate *P* values. Ct values are listed in table S1. (A) was created with BioRender.com.

could be involved in IGTA/TGTA. Previous studies have indeed suggested that small RNAs (including transfer RNA fragments) (*39*, *40*) as well as long RNAs (*41*) can influence the progeny's phenotype. To investigate whether IGTA/TGTA occurs in a similar manner, for example, through mRNA degradation products and/or their derivatives, we isolated total RNA from oocytes, sperm, and testes of wild-type strain and *alcama*$^{ptc/+}$ zebrafish and injected them into one-cell stage zebrafish embryos (Fig. 4A). [We chose the *alcama* model because zebrafish oocytes appear to lack *alcamb* pre-mRNA expression (fig. S6, E and F), thereby facilitating the analysis of the effects of total RNA injections on *alcamb* expression.] Notably, we observed significantly elevated *alcamb* pre-mRNA levels 6 hours after injections of total RNA obtained from oocytes, sperm, or testes of *alcama*$^{ptc/+}$ zebrafish compared with injections of total RNA obtained from oocytes, sperm, and testes of wild-type zebrafish, respectively (Fig. 4, B to D). [Because we were analyzing expression levels at 6 hpf, we focused on pre-mRNA rather than mRNA in order to avoid looking at any remaining maternal mRNA]. Together, these data suggest that germline transmission of mutant mRNAs, their degradation products, and/or their derivatives could underlie IGTA.

Furthermore, we raised the embryos injected with total testis RNA to adulthood and analyzed gene expression levels in their offspring (Fig. 4E). We observed significantly increased *alcamb* mRNA levels in 28 hpf embryos from animals injected with total RNA obtained from *alcama*$^{ptc/+}$ testes compared with 28 hpf embryos from animals injected with total RNA obtained from AB testes (Fig. 4F). These data indicate that the acquired TA traits from total testis RNA injections can be epigenetically inherited.

Inheritance of epigenetic marks is associated with the transgenerational inheritance of transcriptional adaptation in zebrafish

To begin to test the role of epigenetic modifications in IGTA/TGTA, we followed up on previous observations that WDR5-mediated deposition of H3K4me3 appears to be involved in TA (*28*, *29*). To examine whether TA-related H3K4me3 modifications are inherited in the next generations, we first checked the available H3K4me3 chromatin immunoprecipitation sequencing (ChIP-seq) dataset in DANIO-CODE (https://danio-code.zfin.org) and found that, at the 512-cell stage (2.75 hpf) (i.e., prior to midblastula transition), *vclb* does not exhibit H3K4me3 enrichment at its promoter (Fig. 5A). We thus performed ChIP coupled with quantitative polymerase chain reaction (qPCR) (ChIP-qPCR) at this stage and observed the enrichment of H3K4me3 at the promoter of the adapting gene *vclb* in second-generation (F2) wild-type embryos from F1 *vcla*$^{+/+}$ incrosses compared with wild types (Fig. 5, B and C). We also performed ChIP-qPCR with the *alcama* model after the onset of zygotic transcription and observed the enrichment of H3K4me3 at the promoter region of the adapting gene *alcamb* in second-generation (F2) wild-type embryos from F1 *alcama*$^{+/+}$ incrosses compared with wild types (fig. S9). Thus, in addition to the possible germline transmission of mutant mRNAs, their degradation products, and/or their derivatives, IGTA/TGTA could also, in principle, be achieved via the inheritance of epigenetic marks (Fig. 5D), and additional studies will be required to determine the role of these epigenetic marks in IGTA/TGTA.

DISCUSSION

This study shows that the TA response can be inherited over multiple generations. We report that a mutation in a parental genome can lead to transcriptional modulation in wild-type offspring. Observing TGTA in both *C. elegans* and zebrafish models indicates that this phenomenon, as well as its underlying mechanisms, may be common among metazoans. In addition to the well-documented impact of physiological and environmental factors on TEI (*3*, *11*, *15*, *24*–*27*), these data indicate that genetic alterations in a parental genome can also influence the transcriptional landscape of the offspring. Thus, our study calls for even greater attention when designing experiments to examine phenotypic changes in mutants, as the transcriptome of their wild-type siblings may also be affected by mutations in their ancestors' genome.

TEI is most often transmitted through the germline as a direct consequence of physiological or environmental factors, although an alternative model, one that has received increasing attention, postulates that somatic cells are capable of transferring heritable information to the gametes and thereby to progeny (*7*). In the past decade, studies in several model organisms have provided evidence of RNA-mediated soma-to-germline communication during spermatogenesis (*42*–*47*). In mammals, for instance, subpopulations of epididymis small RNAs are selectively packaged into epididymosomes, microvesicles present in the epididymal fluid with functions in sperm maturation and storage (*48*); however, the underlying mechanisms are currently unknown (*49*–*52*). In zebrafish and amphibians,

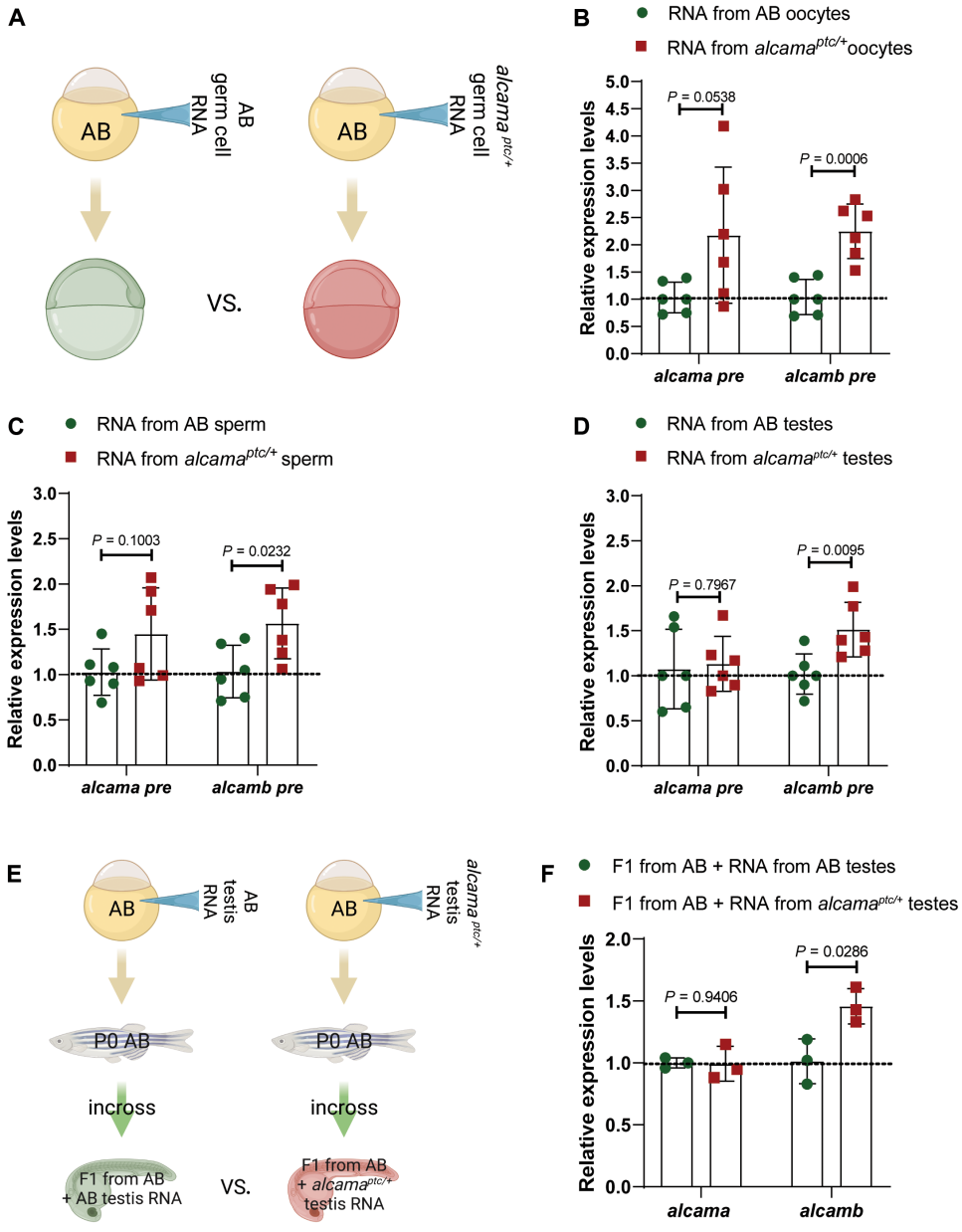

Fig. 4. Injection of total RNA from *alcama*$^{ptc/+}$ germ cells triggers TA, which is also observed in the next generation. (**A**) Schematic representation of the experimental setup. (**B**) Relative pre-mRNA levels of *alcama* and *alcamb* in 6 hpf AB embryos injected with total RNA isolated from oocytes of wild types and *alcama*$^{ptc/+}$ zebrafish. (**C**) Relative pre-mRNA levels of *alcama* and *alcamb* in 6 hpf AB embryos injected with total RNA isolated from sperm of wild types and *alcama*$^{ptc/+}$ zebrafish. (**D**) Relative pre-mRNA levels of *alcama* and *alcamb* in 6 hpf AB embryos injected with total RNA isolated from testes of wild types and *alcama*$^{ptc/+}$ zebrafish. (**E**) Schematic representation of the experimental setup. (**F**) Relative mRNA levels of *alcama* and *alcamb* in 28 hpf F1 offspring from AB zebrafish injected at the one-cell stage with total RNA isolated from testes of wild types and *alcama*$^{ptc/+}$ zebrafish. $n \geq 3$ biologically independent samples. Control expression levels were set at 1. Data are means ± SD, and a two-tailed Student's *t* test was used to calculate *P* values. *C*t values are listed in table S1. (A) and (E) were created with BioRender.com.

spermatogenesis happens through Sertoli-germ cell interactions (*53*), which could allow for soma-to-germline communication. In this study, we showed that a germline-specific mutation in *aldh1a2* in zebrafish is sufficient to induce TA in wild-type offspring (Fig. 3), indicating that, at least for this gene, which is expressed in germ cells, mutations in somatic tissues are not necessary for this process. It is of course likely that for genes not expressed in germ cells, mutations in somatic cells are necessary to induce IGTA. Additional experiments will be required to investigate this question and also to determine how the potential transfer of information occurs between the soma and the germline.

Paramutation is an IEI/TEI-like phenomenon observed in plants (*21*, *53*), *C. elegans* (*22*), and *Drosophila* (*23*); yet, examples in vertebrates are limited. One example of paramutation in mammals is provided by the *Kit*^{tm1Alf} mouse. Wild-type progeny of *Kit*$^{tm1Alf/+}$ mice display the same white tail tip phenotype as their heterozygous parents (*19*). Notably, this phenotype has been attributed to the inheritance of RNA decay fragments from the *Kit* locus. In addition,

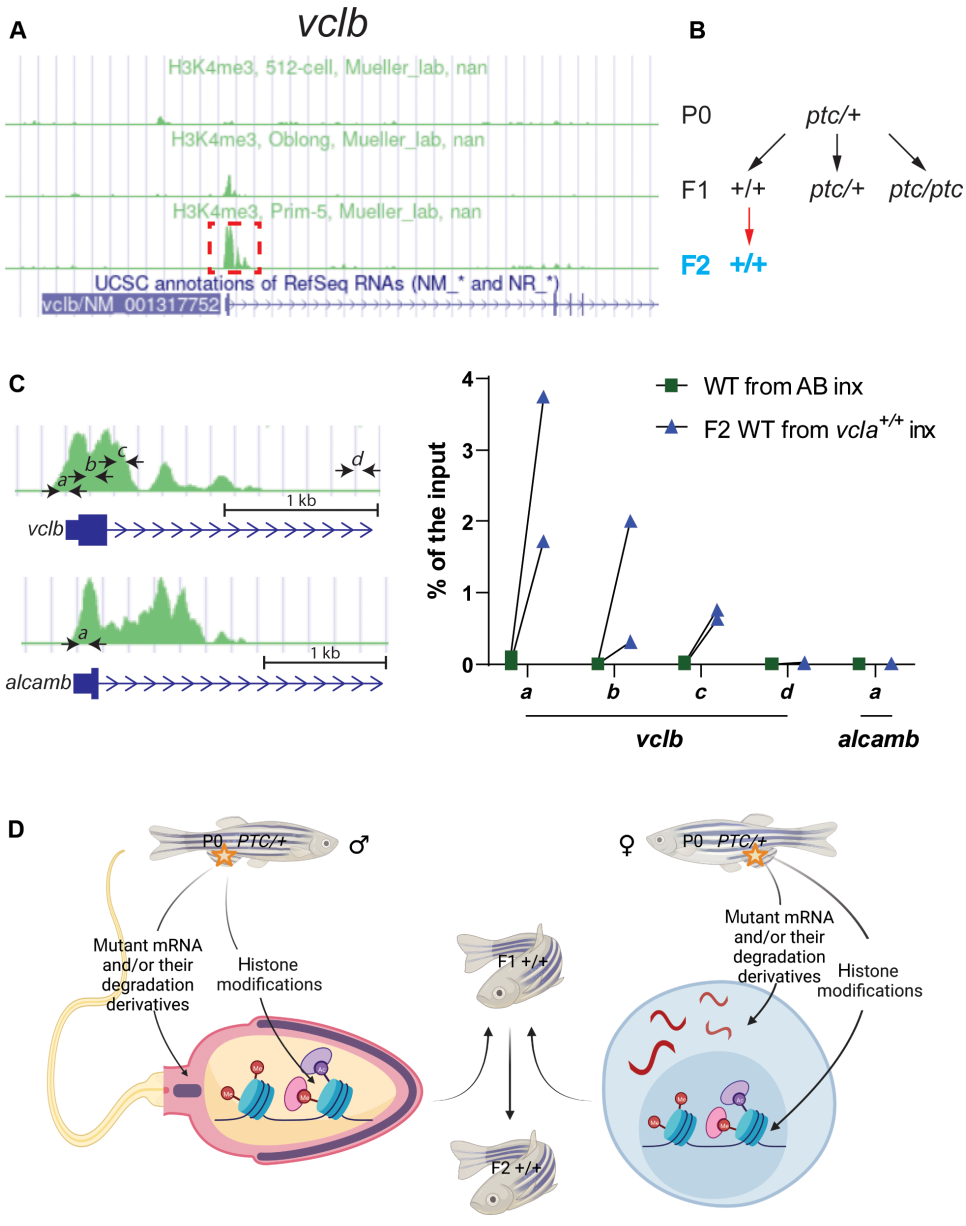

Fig. 5. TGTA in zebrafish is associated with H3K4me3 histone marks. (**A**) Peaks of H3K4me3 ChIP-seq at the *vclb* locus at different stages (obtained from DANIO-CODE). Red boxed area was enlarged in (C) to show the relative location of the ChIP–qPCR primers marked by black arrows (also at the *alcamb* locus, which is used as an external/specificity control). (**B**) Genetic crosses were used to obtain F2 wild-type offspring from heterozygous zebrafish. Black arrows indicate heterozygous intercrosses (intx); red arrow indicates subsequent wild-type incrosses (inx). (**C**) ChIP-qPCR analysis of H3K4me3 occupancy near exon 1 of *vclb* in 512 cell stage wild-type embryos from incrosses of F1 $vcla^{+/+}$ (i.e., wild types from $vcla^{ptc/+}$ intercrosses) compared with wild-type embryos from AB incrosses. Green peaks in *vclb* and *alcamb* loci represent prim-5 stage (24 hpf) H3K4me3 ChIP-seq data obtained from DANIO-CODE. Scale bars, 1 kb. $n = 2$ biologically independent samples. *C*t values are listed in table S1. (**D**) Proposed model of intergenerational and transgenerational inheritance of TA (IGTA and TGTA). Mutant mRNAs, their degradation products (or their derivatives), and/or histone modifications are transmitted through the germline, leading to TA in the offspring. Additional mechanisms are likely to be involved in IGTA and TGTA. PTC, premature termination codon. (D) was created with BioRender.com.

another $Kit^{W\text{-}v}$ missense mutation (which is unlikely to cause mutant mRNA degradation) does not lead to the white tail tip phenotype in the wild-type progeny (*19*, *55*). The apparent requirement of mutant mRNA degradation in this paramutation example suggests that IGTA/TGTA might be at play.

We have previously observed that TA is triggered by mutant mRNA degradation in zebrafish, mouse cells in culture, and nematodes (*28*, *30*). Furthermore, factors involved in small RNA biogenesis and transport are required for the TA response in *C. elegans* (*30*). In the current study, we observed TA in wild-type animals injected with total RNA from germ cells of TA-displaying heterozygous zebrafish as well as in their offspring (Fig. 4). These data are consistent with a model whereby the intergenerational inheritance of the TA response from P0 to F1 animals requires the mutant mRNA, its degradation

products, and/or their derivatives, that are inherited through the germline (Fig. 5D). Since we observed an enrichment of H3K4me3 at the promoter region of the adapting genes *vclb* and *alcamb* in F2 wild-type offspring (Fig. 5C and fig. S9), an additional model involves the inheritance of histone modifications (Fig. 5D), themselves possibly induced by mutant mRNA degradation products, and/or their derivatives.

MATERIALS AND METHODS

C. elegans resource table

All *C. elegans* strains used in this study are found in Table 1.

C. elegans culture conditions and strains

All *C. elegans* strains were kept on 6-cm plates with nematode growth medium agar (*56*) and fed with a lawn of OP50 *Escherichia coli* grown in 500 µl of LB, except for mating plates where the worms were kept on nematode growth medium plates with a lawn of OP50 *E. coli* grown in 150 µl of LB. All *C. elegans* strains used in this study are listed in Table 1. Cultures were maintained at 18° to 20°C. In addition, to minimize the potential for laboratory evolution of the trait, a new culture of the strains was revived at least annually from frozen stocks. All plates with fungal or bacterial contamination were excluded from the experiments.

C. elegans transgenic generation

The DYSSi1000 Mos1-mediated single-copy insertion line was generated as described (*31*) using the EG6699 strain for integration of the *eft-3p::act-5(ptc)::tbb-2 3′UTR* transgene into chromosome 2. Injections to generate the RFP reporter lines DYSSi1001 and DYSEx1002 were performed as described (*57*, *58*), with the following modifications: Plasmids were purified twice using the FastGene Plasmid Mini Kits (Nippon Genetics, FG-90402) and injected at a final total concentration of 100 ng/µl. DYSSi1001 and DYSEx1002 lines were generated by injecting a mixture of *act-3p::rfp* (90 ng/µl) and *sur-5::GFP* (10 ng/µl) plasmids into DYSSi1000 and N2 worms, respectively.

C. elegans construct generation

The overexpression vector *[eft-3p::act-5(ptc)::tbb-2 3′UTR]* was designed to express a PTC-bearing transcript matching the endogenous *dt2019* mutant transcript and was generated by standard restriction enzyme and Gibson cloning methods using N2 genomic DNA as the template. The following primers 5′-ATCGATGCACCTTTGGTCTTTTATTGTCAAC-3′ and 5′-GTTAACTGTTTCCCAACTGAAAAAAAAACAATTTAAT-3′ were used to amplify the *eft-3* promoter region, primers 5′-TTTTTCAGTTGGGAAACAGTTAACGATGGAAGAAGAAATCGCCGC-3′ and 5′-GAAAGGATCTTGCATTTATCAACTAGTCTAAGCCTAAAAAACAAAAACTCCACACG-3′ were used to amplify the complete *act-5* sequence from the ATG to the end of the 3′UTR including introns, and primers 5′-ACTAGTTGATAAATGCAAGATCCTTTCAAGCATTC-3′ and 5′-TTACCGGTGGGAAAAGTTAATTAAGACTTTTTTCTTGGCGGCAC-3′ were used to amplify the *tbb2 3′UTR* to ensure proper termination of the resulting transcript. These amplicons were subsequently assembled into an intermediate vector. The *act-5(PTC)* single-nucleotide polymorphism matching the original *dt2019* mutation (*30*) was generated by point mutagenesis using primers 5′-GAGAAAATCTGGCATCACACATTCTAC-3′ and 5′-CATATCATCtCAGTTGGTGACG-3′. The complete *p-eft-3:act-5(ptc):tbb2 3′UTR* sequence was subsequently cloned into the Mos1 integration vector pBN449 (Addgene, plasmid no. 129555) between the Nhe I and Xma I restriction sites.

C. elegans crossing scheme

N2 males were crossed with DYS0015 (*act-5(dt2019);Ex0002[act-3p::rfp]*) virgin hermaphrodites. The following day, males were removed from the mating plates, and the progeny was subsequently screened for RFP-positive individuals. A subset of the RFP-positive hermaphrodites was isolated for a day to lay eggs prior to genotyping. After identifying the wild-type nematodes, the plates with the eggs from these individuals were kept for further screening. After each generation, single nematodes were isolated to new plates, and their progeny were screened in the same manner. Crosses with DYSSiEx1001 animals were performed in the same manner: *Si[eft-3p::act-5(ptc)](tg/+);Ex1001[act-3p::rfp]* nematodes were obtained from crossing *Si[eft-3p::act-5(ptc)](tg/tg);Ex1001[act-3p::rfp]* virgin hermaphrodites with N2 males. The primer sequences used for genotyping are listed in table S2.

Zebrafish husbandry

All zebrafish (*Danio rerio*, wild-type strains: TL and AB) were maintained under standard conditions according to institutional (Max Planck Society) and national ethical and animal welfare guidelines approved by the Ethics Committee for Animal Experiments at the Regierungspräsidium Darmstadt, Germany (permit numbers: B2/1218 and B2/2023) as well as the Federation of European Laboratory Animal Science Associations guidelines (*59*). Most experiments were performed on zebrafish embryos between 6 and 28 hpf. We used the

Table 1. *C. elegans* resource table.

Reagent type	Designation	Source or reference	Additional information
Strain, strain background	N2	Caenorhabditis Genetics Center, Bristol strain	Wild type
Strain, strain background	DYS0005	(*30*)	*act-5(dt2019)*
Strain, strain background	DYS0014	(*30*)	*Ex0002[act-3p::rfp]*
Strain, strain background	DYS0015	(*30*)	*act-5(dt2019);Ex0002[act-3p::rfp]*
Strain, strain background	EG6699	Caenorhabditis Genetics Center	Wild type for Mos1 integration
Strain, strain background	DYSSi1000	This study	*Si1000[eft-3p::act-5(ptc)::tbb-2 3′UTR]*
Strain, strain background	DYSSi1001	This study	*Si1000[eft-3p::act-5(ptc)::tbb-2 3′UTR];Ex1001[act-3p::rfp]*
Strain, strain background	DYSEx1002	This study	*Ex1000[act-3p::rfp]*

PTC-bearing alleles [*alcama*^{bns201} (*28*), *egfl7*^{s981} (*33*), *aldh1a2*^{tpl137} (*34*), and *vcla*^{bns241} (*28*)] and the RNA-less alleles [*alcama*^{bns244} (*28*) and *egfl7*^{bns302} (*28*)]. All alleles were maintained in the AB background with the exception of *aldh1a2*^{tpl137}, which was generated and maintained in the TL background, and *alcama*^{bns201}, which was in a mixed background. As previously reported, mild up-regulation of *emilin2a* was observed in the *egfl7*$^{RNA\text{-}less}$ allele when compared with *egfl7*$^{+/+}$ siblings (*28*), likely a result of the loss of Egfl7 protein function; a similar up-regulation of *emilin2a* was observed in wild-type offspring from *egfl7* RNA-less allele heterozygous intercrosses. Most zebrafish embryos were obtained from single pair matings. To help keep track of the various matings performed, we refer to matings between animals with the same heterozygous genotype as intercrosses and matings between animals with the same homozygous genotype as incrosses (e.g., https://zfin.org/zf_info/glossary.html#i).

Engineering and validation of the zebrafish *aldh1a2*^{tpl146} (floxed) allele

We established a homozygous line for the intron 7 loxP site (*aldh1a2*^{tpl139}; fig. S2C) (*34*) and injected embryos with *aldh1a2* single-guide RNA (sgRNA), *Cas9* mRNA, and an Homology-directed repair (HDR) template oligonucleotide using a published methodology (*34*). We identified an F0 that transmitted the integration of the second loxP site in the germline and verified the allele by screening individual F1 embryos (two embryos out of six screened were positive). Sibling F1s were raised to adulthood and screened for intron 8 loxP site by fin biopsy PCR and sequencing. One of the 13 zebrafish screened was found to contain a precise integration of the additional loxP site. To validate this newly engineered floxed *aldh1a2*^{tpl146} allele, this F1 zebrafish was crossed to the previously reported exon 8 deletion mutant *aldh1a2*^{tpl137} (*34*), and embryos were injected with *Cre* mRNA to induce excision of the eighth exon. All uninjected larvae were phenotypically normal at 72 hpf (n = 174), indicating that the floxed allele is functionally wild type. Approximately one-quarter of the *Cre*-injected larvae (38 of 136, 27.9%) displayed phenotypes consistent with the complete loss of *aldh1a2* function, including the loss of mesodermal head tissue, pericardial edema, tail curvature, and the absence of pectoral fins. Sixteen *Cre*-injected larvae (eight phenotypically mutant and eight phenotypically wild type) were genotyped by PCR. All eight phenotypically mutant larvae were found to be transheterozygous for the *aldh1a2*^{tpl137} deletion allele and *Cre*-deleted floxed *aldh1a2*^{tpl146} allele, while all eight phenotypically wild-type larvae were found to contain at least one wild-type allele. *Cre*-mediated excision of exon 8 was confirmed by sequencing the PCR fragment. The *aldh1a2*^{tpl146} allele was generated and maintained in the TL background. The sequences of the oligos used for mutagenesis and genotyping are listed in table S2.

Genome editing by CRISPR-Cas9

CRISPR gRNA design was performed using the online tools (https://eu.idtdna.com/site/order/designtool/index/CRISPR_SEQUENCE and http://chopchop.cbu.uib.no/). gRNAs were generated with gRNA-specific primers (Thermo Fisher Scientific) as described (*60*). The gRNAs were transcribed with the MEGAshortscript T7 Transcription Kit (Thermo Fisher Scientific), followed by purification with the RNA Clean & Concentrator Kit (Zymo Research). The *vcla* full locus deletion allele (*vcla*^{bns605}) was generated with a pair of gRNAs as illustrated in fig. S3C. All gRNAs used for CRISPR-Cas9 genome editing are listed in table S2.

Genotyping

DNA and RNA were extracted from at least 24 individual embryos using TRIzol (Invitrogen) followed by phenol-chloroform extraction. In brief, single embryos were lysed and homogenized in 100 μl of TRIzol using a Next Advance Bullet Blender Homogenizer (Scientific Instrument Services). Twenty microliters of chloroform was then added, and phase separation was obtained following vortexing and centrifugation. The aqueous phase (containing RNA) was isolated and stored at −80°C, and the organic phase (containing DNA) was subjected to ethanol purification to precipitate the DNA. Purified DNA was then dissolved in Tris-EDTA buffer containing 1% proteinase K (Thermo Fisher Scientific) for genotyping. RNAs from genotyped zebrafish were then pooled for further purification and cDNA synthesis with the exception of the experiments shown in figs. S2D, S3E, and S8E, which were performed with a single-embryo RNA. For each experiment, these steps were performed on embryos from at least three different crosses. High-resolution melt analysis (*61*) was used to genotype all zebrafish alleles, with the exception of the *aldh1a2*^{tpl137} and *aldh1a2*^{tpl146} alleles, which were genotyped by PCR. The primer sequences used for genotyping are listed in table S2.

RT-qPCR analysis

Reverse transcription (RT)–qPCR was performed using a CFX Connect Real-Time System (Bio-Rad). *C. elegans* RNA was isolated as described (*62*). RNAs from five synchronized early larval stage worms were pooled. For RT, SuperScript III reverse transcriptase (Invitrogen) was used following the manufacturer's instructions. Zebrafish RNA was isolated using TRIzol, and at least 500 ng of RNA was used for RT. cDNA synthesis was performed using the Maxima First Strand cDNA Synthesis Kit (Thermo Fisher Scientific). All reactions were performed in at least technical duplicates, and the results usually represent biological triplicates; when the biological replicates were too variable to assess TGTA, additional ones were analyzed. RT-qPCR was performed at the embryonic stage when the wild-type version of the mutated gene exhibits its highest level of expression. *rpl13a* was used as a reference gene for all zebrafish experiments; *cdc42* was used as a reference gene for all *C. elegans* experiments. Primer sequences used for the RT-qPCR experiments are listed in table S2. Fold changes were calculated using the $2^{-\Delta\Delta Ct}$ method. All *C*t values are listed in table S1. *C*t values for the reference genes ranged between 12 and 26.

In vitro transcription and microinjections

sgRNAs were transcribed with the MEGAshortscript T7 Transcription Kit, followed by purification using the RNA Clean & Concentrator Kits. The pT3TSnCas9n (Addgene, plasmid no. 46757) plasmid (*63*) was linearized using Xba I [New England Biolabs (NEB)]; capped Cas9 mRNA was synthesized using the mMESSAGE mMACHINE T3 Transcription Kit (Thermo Fisher Scientific) and purified using the RNA Clean & Concentrator Kits. A cDNA corresponding to *aldh1a2* full-length mRNA was amplified using whole-embryo cDNA as a template. PCR fragments were ligated into a pCS2^{+} vector between the Bam HI and Xba I (NEB) sites. Zebrafish codon-modified Cre recombinase was amplified from pCS2-Cre (gift from H. Burgess; Addgene, plasmid no. 61391) (*64*). Plasmids were linearized using Not I–HF (NEB) and in vitro transcribed using the mMESSAGE mMACHINE SP6 Transcription Kit. RNA was then purified using the RNA Clean & Concentrator Kits. A total of 75 pg of *aldh1a2* full-length mRNA was injected into embryos from heterozygous

intercrosses at the one-cell stage. A total of 100 pg of *Cre* mRNA was injected into embryos from heterozygous intercrosses at the one-cell stage. To generate the *vasa-Cre-nos1* 3′UTR plasmid, zebrafish codon-modified Cre recombinase was amplified from pCS2-Cre (*63*) and cloned into a *vasa-mGFP-nos1* 3′UTR plasmid (gift from E. Raz) (*65*). Plasmids were linearized using Not I–HF (NEB) and in vitro transcribed using the mMESSAGE mMACHINE SP6 Transcription Kit. RNA was then purified using the RNA Clean & Concentrator Kits. A total of 100 pg of *vasa-GFP-nos1 3′UTR* mRNA plus 0.6 ng of standard control morpholino or *dnd1* morpholino were injected into embryos from AB incrosses and from *alcama*$^{bns201/+}$ intercrosses at the one-cell stage. A total of 100 pg of *vasa-GFP-nos1 3′UTR* mRNA plus 10 pg of *vasa-cre-nos1 3′UTR* mRNA were injected into *aldh1a2*$^{tpl146/+}$ intercrosses at the one-cell stage to create a germline-specific mutation.

Germline RNA preparation

Egg and sperm isolation and testis dissection were performed as described (*66*). Total RNA was extracted using TRIzol, followed by phenol-chloroform extraction. A total of 100 pg of total RNA was injected into embryos from AB incrosses at the one-cell stage. We raised embryos injected with total RNA from oocytes, sperm, and testes but only had enough surviving adults from the testis RNA-injected ones to carry out the experiments shown in Fig. 4E.

Sample preparation and cell sorting

Zebrafish embryos were obtained from *aldh1a2*$^{tpl146/+}$ intercrosses, followed by 100 pg of *vasa-GFP-nos1 3′UTR* mRNA plus 10 pg of *vasa-Cre-nos1 3′UTR* mRNA injections at the one-cell stage. At 24 hpf, dechorionated embryos were dissociated with Liberase Blendzyme (Roche) and prepared as described (*67*) with the following modifications: Incubation was performed at 30°C with gentle shaking for 40 min, followed by careful resuspension in 1× Hanks' balanced salt solution, 0.25% bovine serum albumin, and 10 mM Hepes buffer. The resuspended cells were immediately sorted using a BD FACSAria III (BD) sorter for green fluorescent protein $(GFP)^+$/4′,6-diamidino-2-phenylindole $(DAPI)^-$ cells. Debris and clumps were excluded using the FSC/SSC parameters. Dead cells were excluded by selecting against DAPI-positive cells, which were detected using laser excitation at 405 nm and emission at 450/40 nm. GFP-labeled cells were detected using laser excitation at 488 nm and emission at 530/30 nm. The sort gate for live GFP-positive cells was defined on the basis of the GFP-negative control.

RNA metabolic labeling

Metabolic labeling was performed as described (*28*, *68*, *69*). In brief, at 24 and 28 hpf, dechorionated zebrafish embryos were treated with 25 ml of 200 μM 4-thiouridine (4sU; Sigma-Aldrich) for 1 hour, followed by phenol-chloroform total RNA extraction. A total of 80 μg of RNA was incubated with biotin-HPDP (Thermo Fisher Scientific) to specifically biotinylate the newly transcribed 4sU-labeled RNAs. Biotinylated RNAs were then pulled down using the μMACS Streptavidin Kit (Miltenyi), and the same amount of pulled-down RNA was used for RT and downstream qPCR analysis. This experiment was performed three times.

Chromatin immunoprecipitation

ChIP was performed using the truChIP Chromatin Shearing Reagent Kit (Covaris) using 500 embryos per immunoprecipitation according to the manufacturer's instructions. Chromatin was sheared using a Bioruptor (Diagenode) to generate fragments of 200 to 400 base pairs in size. Immunoprecipitation was then performed as described (*70*). The following antibodies were used: rabbit immunoglobulin G (3 μl per immunoprecipitation; Thermo Fisher Scientific, 026102) and H3K4me3 (4 μl per immunoprecipitation; Cell Signaling Technology, no. 9751, lot 14). Following immunoprecipitation and reverse crosslinking, samples were purified using ethanol purification. Because of the challenges associated with collecting enough embryos for the ChIP-qPCR experiments, they were only performed twice.

Confocal microscopy

Fluorescence images of *C. elegans* were acquired using a Zeiss LSM 700 confocal microscope (Plan-Apochromat 10×/0.45 objective lens). Worms were mounted immobilized in polystyrene microbeads as described (*71*). Fluorescence images of zebrafish embryos were acquired using a Zeiss LSM 700 confocal microscope (Plan-Apochromat 10×/0.45 objective lens). Embryos were mounted in 1% UltraPure Low Melting Point Agarose (Thermo Fisher Scientific) in egg water with tricaine in a glass-bottomed petri dish (MatTek). Obtained images were subsequently processed with the ZEN software (black edition). All figures were prepared using Adobe Photoshop 2022 and Adobe Illustrator 2022.

Statistics and reproducibility

No statistical methods were used to predetermine the sample size. The experiments were not randomized. The investigators were not blinded to allocation during experiments and outcome assessment. All experiments were performed at least twice with three biological replicates each time/in total of six biological replicates, unless otherwise noted. Statistical analysis was performed using GraphPad Prism 9. Data are means ± SD, and a two-tailed Student's *t* test was used to calculate *P* values with the exception of the data shown in fig. S5, which were analyzed with a two-tailed paired *t* test of the ΔΔCt. $P < 0.05$ was considered as statistically significant.

SUPPLEMENTARY MATERIALS

Supplementary material for this article is available at https://science.org/doi/10.1126/sciadv.abj2029

View/request a protocol for this paper from *Bio-protocol*.

REFERENCES AND NOTES

1. K. Skvortsova, N. Iovino, O. Bogdanovic, Functions and mechanisms of epigenetic inheritance in animals. *Nat. Rev. Mol. Cell Biol.* **19**, 774–790 (2018).
2. E. J. Richards, Inherited epigenetic variation–Revisiting soft inheritance. *Nat. Rev. Genet.* **7**, 395–401 (2006).
3. L. Daxinger, E. Whitelaw, Understanding transgenerational epigenetic inheritance via the gametes in mammals. *Nat. Rev. Genet.* **13**, 153–162 (2012).
4. E. A. Miska, A. C. Ferguson-Smith, Transgenerational inheritance: Models and mechanisms of non-DNA sequence-based inheritance. *Science* **354**, 59–63 (2016).
5. M. Toth, Mechanisms of non-genetic inheritance and psychiatric disorders. *Neuropsychopharmacology* **40**, 129–140 (2015).
6. E. Heard, R. A. Martienssen, Transgenerational epigenetic inheritance: Myths and mechanisms. *Cell* **157**, 95–109 (2014).
7. M. F. Perez, B. Lehner, Intergenerational and transgenerational epigenetic inheritance in animals. *Nat. Cell Biol.* **21**, 143–151 (2019).
8. J. J. Tuscher, J. J. Day, Multigenerational epigenetic inheritance: One step forward, two generations back. *Neurobiol. Dis.* **132**, 104591 (2019).
9. N. O. Burton, E. L. Greer, Multigenerational epigenetic inheritance: Transmitting information across generations. *Semin. Cell Dev. Biol.* **127**, 121–132 (2022).
10. N. Iwanam, D. F. Lawir, K. Sikora, C. O'Meara, K. Takeshita, M. Schorpp, T. Boehm, Transgenerational inheritance of impaired larval T cell development in zebrafish. *Nat. Commun.* **11**, 4505 (2020).

11. V. Serobyan, R. J. Sommer, Developmental systems of plasticity and trans-generational epigenetic inheritance in nematodes. *Curr. Opin. Genet. Dev.* **45**, 51–57 (2017).
12. I. Lev, U. Seroussi, H. Gingold, R. Bril, S. Anava, O. Rechavi, MET-2-dependent H3K9 methylation suppresses transgenerational small RNA inheritance. *Curr. Biol.* **27**, 1138–1147 (2017).
13. L. Duempelmann, M. Skribbe, M. Buhler, Small RNAs in the transgenerational inheritance of epigenetic information. *Trends Genet.* **36**, 203–214 (2020).
14. V. Cavalieri, G. Spinelli, Environmental epigenetics in zebrafish. *Epigenetics Chromatin* **10**, 46 (2017).
15. Q. L. Wan, X. Meng, W. Dai, Z. Luo, C. Wang, X. Fu, J. Yang, Q. Ye, Q. Zhou, N6-methyldeoxyadenine and histone methylation mediate transgenerational survival advantages induced by hormetic heat stress. *Sci. Adv.* **7**, (2021).
16. Z. Paroo, Q. Liu, X. Wang, Biochemical mechanisms of the RNA-induced silencing complex. *Cell Res.* **17**, 187–194 (2007).
17. D. Holoch, D. Moazed, RNA-mediated epigenetic regulation of gene expression. *Nat. Rev. Genet.* **16**, 71–84 (2015).
18. D. L. Yang, G. Zhang, K. Tang, J. Li, L. Yang, H. Huang, H. Zhang, J. K. Zhu, Dicer-independent RNA-directed DNA methylation in *Arabidopsis*. *Cell Res.* **26**, 66–82 (2016).
19. M. Rassoulzadegan, V. Grandjean, P. Gounon, S. Vincent, I. Gillot, F. Cuzin, RNA-mediated non-mendelian inheritance of an epigenetic change in the mouse. *Nature* **441**, 469–474 (2006).
20. S. Yuan, D. Oliver, A. Schuster, H. Zheng, W. Yan, Breeding scheme and maternal small RNAs affect the efficiency of transgenerational inheritance of a paramutation in mice. *Sci. Rep.* **5**, 9266 (2015).
21. V. L. Chandler, Paramutation: From maize to mice. *Cell* **128**, 641–645 (2007).
22. A. Sapetschnig, P. Sarkies, N. J. Lehrbach, E. A. Miska, Tertiary siRNAs mediate paramutation in *C. elegans*. *PLOS Genet.* **11**, e1005078 (2015).
23. A. de Vanssay, A. L. Bougé, A. Boivin, C. Hermant, L. Teysset, V. Delmarre, C. Antoniewski, S. Ronsseray, Paramutation in *Drosophila* linked to emergence of a piRNA-producing locus. *Nature* **490**, 112–115 (2012).
24. S. Kishimoto, M. Uno, E. Okabe, M. Nono, E. Nishida, Environmental stresses induce transgenerationally inheritable survival advantages via germline-to-soma communication in *Caenorhabditis elegans*. *Nat. Commun.* **8**, 14031 (2017).
25. K. H. Seong, D. Li, H. Shimizu, R. Nakamura, S. Ishii, Inheritance of stress-induced, ATF-2-dependent epigenetic change. *Cell* **145**, 1049–1061 (2011).
26. R. A. Brink, E. D. Styles, J. D. Axtell, Paramutation: Directed genetic change. Paramutation occurs in somatic cells and heritably alters the functional state of a locus. *Science* **159**, 161–170 (1968).
27. A. Constantinof, L. Boureau, V. G. Moisiadis, A. Kostaki, M. Szyf, S. G. Matthews, Prenatal glucocorticoid exposure results in changes in gene transcription and DNA methylation in the female juvenile guinea pig hippocampus across three generations. *Sci. Rep.* **9**, 18211 (2019).
28. M. A. El-Brolosy, Z. Kontarakis, A. Rossi, C. Kuenne, S. Günther, N. Fukuda, K. Kikhi, G. L. Boezio, C. M. Takacs, S. L. Lai, R. Fukuda, C. Gerri, A. J. Giraldez, D. Y. R. Stainier, Genetic compensation triggered by mutant mRNA degradation. *Nature* **568**, 193–197 (2019).
29. Z. Ma, P. Zhu, H. Shi, L. Guo, Q. Zhang, Y. Chen, S. Chen, Z. Zhang, J. Peng, J. Chen, PTC-bearing mRNA elicits a genetic compensation response via Upf3a and COMPASS components. *Nature* **568**, 259–263 (2019).
30. V. Serobyan, Z. Kontarakis, M. A. El-Brolosy, J. M. Welker, O. Tolstenkov, A. M. Saadeldein, N. Retzer, A. Gottschalk, A. M. Wehman, D. Y. Stainier, Transcriptional adaptation in *Caenorhabditis elegans*. *eLife* **9**, e50014 (2020).
31. C. Frokjaer-Jensen, M. Wayne Davis, C. E. Hopkins, B. J. Newman, J. M. Thummel, S. P. Olesen, M. Grunnet, E. M. Jorgensen, Single-copy insertion of transgenes in *Caenorhabditis elegans*. *Nat. Genet.* **40**, 1375–1383 (2008).
32. L. D. Mathies, S. Ray, K. Lopez-Alvillar, M. N. Arbeitman, A. G. Davies, J. C. Bettinger, mRNA profiling reveals significant transcriptional differences between a multipotent progenitor and its differentiated sister. *BMC Genomics* **20**, 427 (2019).
33. A. Rossi, Z. Kontarakis, C. Gerri, H. Nolte, S. Hölper, M. Krüger, D. Y. Stainier, Genetic compensation induced by deleterious mutations but not gene knockdowns. *Nature* **524**, 230–233 (2015).
34. L. Burg, N. Palmer, K. Kikhi, E. S. Miroshnik, H. Rueckert, E. Gaddy, C. MacPherson Cunningham, K. Mattonet, S. L. Lai, R. Marin-Juez, R. B. Waring, D. Y. Stainier, D. Balciunas, Conditional mutagenesis by oligonucleotide-mediated integration of loxP sites in zebrafish. *PLOS Genet.* **14**, e1007754 (2018).
35. Y. Liu, M. E. Kossack, M. E. McFaul, L. N. Christensen, S. Siebert, S. R. Wyatt, C. N. Kamei, S. Horst, N. Arroyo, I. A. Drummond, C. E. Juliano, B. W. Draper, Single-cell transcriptome reveals insights into the development and function of the zebrafish ovary. *eLife* **11**, e76014 (2022).
36. M. Doitsidou, M. Reichman-Fried, J. Stebler, M. Köprunner, J. Dörries, D. Meyer, C. V. Esguerra, T. Leung, E. Raz, Guidance of primordial germ cell migration by the chemokine SDF-1. *Cell* **111**, 647–659 (2002).
37. U. Wolke, G. Weidinger, M. Koprunner, E. Raz, Multiple levels of posttranscriptional control lead to germ line-specific gene expression in the zebrafish. *Curr. Biol.* **12**, 289–294 (2002).
38. B. Ciruna, G. Weidinger, H. Knaut, B. Thisse, C. Thisse, E. Raz, A. F. Schier, Production of maternal-zygotic mutant zebrafish by germ-line replacement. *Proc. Natl. Acad. Sci. U.S.A.* **99**, 14919–14924 (2002).
39. C. C. Conine, F. Sun, L. Song, J. A. Rivera-Perez, O. J. Rando, Small RNAs gained during epididymal transit of sperm are essential for embryonic development in mice. *Dev. Cell* **46**, 470–480.e3 (2018).
40. K. Gapp, E. A. Miska, tRNA fragments: Novel players in intergenerational inheritance. *Cell Res.* **26**, 395–396 (2016).
41. K. Gapp, G. van Steenwyk, P. L. Germain, W. Matsushima, K. L. Rudolph, F. Manuella, M. Roszkowski, G. Vernaz, T. Ghosh, P. Pelczar, I. M. Mansuy, E. A. Miska, Alterations in sperm long RNA contribute to the epigenetic inheritance of the effects of postnatal trauma. *Mol. Psychiatry* **25**, 2162–2174 (2020).
42. A. M. Cunningham, D. M. Walker, A. Ramakrishnan, M. A. Doyle, R. C. Bagot, H. M. Cates, C. J. Peña, O. Issler, C. K. Lardner, C. Browne, S. J. Russo, L. Shen, E. J. Nestler, Sperm transcriptional state associated with paternal transmission of stress phenotypes. *J. Neurosci.* **41**, 6202–6216 (2021).
43. D. Bourc'his, O. Voinnet, A small-RNA perspective on gametogenesis, fertilization, and early zygotic development. *Science* **330**, 617–622 (2010).
44. G. Martinez, K. Panda, C. Kohler, R. K. Slotkin, Silencing in sperm cells is directed by RNA movement from the surrounding nurse cell. *Nat. Plants* **2**, 16030 (2016).
45. U. Sharma, C. C. Conine, J. M. Shea, A. Boskovic, A. G. Derr, X. Y. Bing, C. Belleannee, A. Kucukural, R. W. Serra, F. Sun, L. Song, B. R. Carone, E. P. Ricci, X. Z. Li, L. Fauquier, M. J. Moore, R. Sullivan, C. C. Mello, M. Garber, O. J. Rando, Biogenesis and function of tRNA fragments during sperm maturation and fertilization in mammals. *Science* **351**, 391–396 (2016).
46. U. Sharma, F. Sun, C. C. Conine, B. Reichholf, S. Kukreja, V. A. Herzog, S. L. Ameres, O. J. Rando, Small RNAs are trafficked from the epididymis to developing mammalian sperm. *Dev. Cell* **46**, 481–494.e6 (2018).
47. C. P. Morgan, J. C. Chan, T. L. Bale, Driving the next generation: Paternal lifetime experiences transmitted via extracellular vesicles and their small RNA cargo. *Biol. Psychiatry* **85**, 164–171 (2019).
48. N. A. Trigg, A. L. Eamens, B. Nixon, The contribution of epididymosomes to the sperm small RNA profile. *Reproduction* **157**, R209–R223 (2019).
49. R. Sullivan, Epididymosomes: A heterogeneous population of microvesicles with multiple functions in sperm maturation and storage. *Asian J. Androl.* **17**, 726–729 (2015).
50. C. Belleannee, E. Calvo, J. Caballero, R. Sullivan, Epididymosomes convey different repertoires of microRNAs throughout the bovine epididymis. *Biol. Reprod.* **89**, 30 (2013).
51. J. N. Reilly, E. A. McLaughlin, S. J. Stanger, A. L. Anderson, K. Hutcheon, K. Church, B. P. Mihalas, S. Tyagi, J. E. Holt, A. L. Eamens, B. Nixon, Characterisation of mouse epididymosomes reveals a complex profile of microRNAs and a potential mechanism for modification of the sperm epigenome. *Sci. Rep.* **6**, 31794 (2016).
52. A. Schuster, C. Tang, Y. Xie, N. Ortogero, S. Yuan, W. Yan, SpermBase: A database for sperm-borne RNA contents. *Biol. Reprod.* **95**, 99 (2016).
53. M. C. Leal, P. P. de Waal, Á. García-López, S. X. Chen, J. Bogerd, R. W. Schulz, Zebrafish primary testis tissue culture: An approach to study testis function ex vivo. *Gen. Comp. Endocrinol.* **162**, 134–138 (2009).
54. J. B. Hollick, Paramutation and related phenomena in diverse species. *Nat. Rev. Genet.* **18**, 5–23 (2017).
55. K. Nocka, J. C. Tan, E. Chiu, T. Y. Chu, P. Ray, P. Traktman, P. Besmer, Molecular bases of dominant negative and loss of function mutations at the murine c-kit/white spotting locus: W37, Wv, W41 and W. *EMBO J.* **9**, 1805–1813 (1990).
56. S. Brenner, The genetics of *Caenorhabditis elegans*. *Genetics* **1**, 71–94 (1974).
57. C. C. Mello, J. M. Kramer, D. Stinchcomb, V. Ambros, Efficient gene transfer in *C. elegans*: Extrachromosomal maintenance and integration of transforming sequences. *EMBO J.* **10**, 3959–3970 (1991).
58. C. Mello, A. Fire, Chapter 19 DNA transformation. *Methods Cell Biol.* **48**, 451–482 (1995).
59. P. Alestrom, L. D'Angelo, P. J. Midtlyng, D. F. Schorderet, S. Schulte-Merker, F. Sohm, S. Warner, Zebrafish: Housing and husbandry recommendations. *Lab Anim.* **54**, 213–224 (2020).
60. W. Y. Hwang, Y. Fu, D. Reyon, M. L. Maeder, S. Q. Tsai, J. D. Sander, R. T. Peterson, J. R. Yeh, J. K. Joung, Efficient genome editing in zebrafish using a CRISPR-Cas system. *Nat. Biotechnol.* **31**, 227–229 (2013).
61. E. Samarut, A. Lissouba, P. Drapeau, A simplified method for identifying early CRISPR-induced indels in zebrafish embryos using high resolution melting analysis. *BMC Genomics* **17**, 547 (2016).
62. K. Ly, S. J. Reid, R. G. Snell, Rapid RNA analysis of individual *Caenorhabditis elegans*. *MethodsX* **2**, 59–63 (2015).

63. L. E. Jao, S. R. Wente, W. Chen, Efficient multiplex biallelic zebrafish genome editing using a CRISPR nuclease system. *Proc. Natl. Acad. Sci. U.S.A.* **110**, 13904–13909 (2013).
64. E. J. Horstick, D. C. Jordan, S. A. Bergeron, K. M. Tabor, M. Serpe, B. Feldman, H. A. Burgess, Increased functional protein expression using nucleotide sequence features enriched in highly expressed genes in zebrafish. *Nucleic Acids Res.* **43**, e48 (2015).
65. K. Dumstrei, R. Mennecke, E. Raz, Signaling pathways controlling primordial germ cell migration in zebrafish. *J. Cell Sci.* **117**, 4787–4795 (2004).
66. M. Westerfield, M. Westernfield, in *The Zebrafish Book: A Guide for the Laboratory Use of Zebrafish (Danio rerio)* (University of Oregon, 2007).
67. D. Traver, B. H. Paw, K. D. Poss, W. T. Penberthy, S. Lin, L. I. Zon, Transplantation and in vivo imaging of multilineage engraftment in zebrafish bloodless mutants. *Nat. Immunol.* **4**, 1238–1246 (2003).
68. B. Radle, A. J. Rutkowski, Z. Ruzsics, C. C. Friedel, U. H. Koszinowski, L. Dölken, Metabolic labeling of newly transcribed RNA for high resolution gene expression profiling of RNA synthesis, processing and decay in cell culture. *J. Vis. Exp.* , 50195 (2013).
69. W. Sun, W. Chen, Metabolic labeling of newly synthesized RNA with 4sU to in parallel assess RNA transcription and decay. *Methods Mol. Biol.* **1720**, 25–34 (2018).
70. R. Blecher-Gonen, Z. Barnett-Itzhaki, D. Jaitin, D. Amann-Zalcenstein, D. Lara-Astiaso, I. Amit, High-throughput chromatin immunoprecipitation for genome-wide mapping of in vivo protein-DNA interactions and epigenomic states. *Nat. Protoc.* **8**, 539–554 (2013).
71. E. Kim, L. Sun, C. V. Gabel, C. Fang-Yen, Long-term imaging of *Caenorhabditis elegans* using nanoparticle-mediated immobilization. *PLOS ONE* **8**, e53419 (2013).

Acknowledgments: We thank S. Capon, C. Cirzi, A. Rossi, T. Bertozzi, Z. Kontarakis, S. Perathoner, L. Xie, and P. Krishnaraj for discussion and comments on the manuscript. We also thank A. Atzberger and K. Kikhi at the MPI Fluorescence-Activated Cell Sorting service group for the support with cell sorting. We thank S. Allanki, K. Mattonet, and S. Howard for technical advice and support and H. Burgess, E. Raz, and P. Askjaer for providing plasmids. The DYSSi1000 Mos1-mediated single-copy insertion line was generated in the Genome Engineering Facility, Max Planck Institute of Molecular Cell Biology and Genetics, Dresden, Germany. We thank the DANIO-CODE consortium (https://danio-code.zfin.org) for providing zebrafish epigenomics data. **Funding:** This research was supported by an award from the Cardio-Pulmonary Institute (EXC 2026, project ID: 390649896) to Z.J.; an Otto Bayer Fellowship from the Bayer Foundation to M.A.E.-B.; and funds from the Max Planck Society, the European Research Council (ERC) under the European Union's Horizon 2020 research and innovation programme (AdG 694455-ZMOD and AdG 101021349-TAaGC), and the Leducq Foundation to D.Y.R.S. **Author contributions:** Conceptualization: Z.J., M.A.E.-B., V.S., and D.Y.R.S. Methodology: Z.J., M.A.E.-B., and V.S. Investigation: All authors. Resources: D.Y.R.S. Writing: Z.J., M.A.E.-B., V.S., and D.Y.R.S, with inputs from all authors. Supervision: D.Y.R.S. Project administration and funding acquisition: D.Y.R.S. **Competing interests:** The authors declare that they have no competing interests. **Data and materials availability:** All data needed to evaluate the conclusions in the paper are present in the paper and/or the Supplementary Materials.

Submitted 27 April 2021
Accepted 12 October 2022
Published 25 November 2022
10.1126/sciadv.abj2029

ScienceAdvances

Parental mutations influence wild-type offspring via transcriptional adaptation

Zhen JiangMohamed A. El-BrolosyVahan SerobyanJordan M. WelkerNicholas RetzerChristopher M. DooleyGabrielius JakutisThomas JuanNana FukudaHans-Martin MaischeinDarius BalciunasDidier Y.R. Stainier

Sci. Adv., 8 (47), eabj2029. • DOI: 10.1126/sciadv.abj2029